Investigation of localized Phase Changes using High Resolution Electron Back-Scatter Diffraction in Thin Film Cadmium Telluride Photovoltaic Material with High Lattice Defect Densities

A Abbas[1], A. Munshi[2], K.L. Barth[2], W.S. Sampath[2], G.D West[3], and J.M. Walls[1],

[1]CREST, Loughborough University, Loughborough, United Kingdom, [2]NSF I/UCRC for Next Generation Photovoltaics, Colorado State University, Fort Collins, United States, University of Warwick, Coventry, United Kingdom

***Abstract* — This study focuses on the microstructural and crystallographic characteristics of cadmium telluride thin film photovoltaics using the novel characterization technique of transmission electron back-scatter diffraction (T-EBSD). Taking advantage of the increase in resolution of transmission electron back-scatter diffraction capabilities, identification of localized changes of phase within the cadmium telluride grains have been detected. T-EBSD of the cadmium telluride grains show areas containing very high defect densities indexed to the hexagonal phase whereas the rest of the grain is indexed to the cubic phase, showing that the high densities of defects alters the stacking formation enough to causes a localized change of phase, forming two different phases within the same grain.**

***Index Terms* — CdTe, PV, $CdCl_2$, TEM, EBSD, T-EBSD**

I. Introduction

Thin film Cadmium Telluride solar cells are the most successful and lowest cost second generation solar technology with current annual production of ~3GW [1]. An essential step in the manufacture of cadmium telluride modules is activation using the cadmium chloride process. This study focuses on the effects of the cadmium chloride treatment on the cadmium telluride interior grain structure. Transmission electron microscopy has revealed high densities of defects in as-deposited cells using all deposition techniques including close space sublimation and vapour transport deposition. Many of these defects are removed during the cadmium chloride activation treatment [2]. The treatment of the cadmium telluride grains results in an almost total reduction in planar defects with few twins remaining in some grains. Following treatment, the cadmium telluride indexes with a high confidence to the cubic zinc blende phase in electron back-scatter diffraction (EBSD) Cadmium telluride grains prior to the cadmium chloride treatment do not index well to a cubic zinc blende phase [3]. Transmission electron back-scatter diffraction (T-EBSD) has a much improved resolution compared to EBSD and is utilized in this study to determine why as-deposited cadmium telluride does not appear cubic as expected.

II. Experimental Details

A. Cadmium Telluride Deposition and the Cadmium Chloride Activation Treatment

The thin film cadmium telluride cells were deposited in a superstrate configuration using close-spaced sublimation (CSS) on NSG-Pilkington TEC10 fluorine doped tin oxide (FTO) coated on 3 mm soda lime glass. A thin layer of cadmium sulphide was deposited onto a plasma cleaned transparent conducting oxide. This was followed by the CSS deposition of the cadmium telluride film. The devices then underwent a previously optimized post deposition cadmium chloride activation treatment [4]. The efficiency of this cell was measured to be above 12%. The cell efficiency before the cadmium chloride treatment was measured to be <1%.

B. Characterization Methods

Samples for Transmission Electron Microscopy (TEM) were prepared by Focused Ion Beam (FIB) milling using a dual beam FEI Nova 600 Nanolab. A standard in situ lift out method was used to prepare cross-sectional samples through the coating into the glass substrate. TEM analysis was carried out using a Tecnai F20 operating at 200 kV to investigate the detailed microstructures of the cell cross sections.

Electron back-scatter diffraction (EBSD) requires a very smooth surface for effective microstructural mapping. Therefore to analyse the surface of the CdTe directly a section of the surface was smoothed with FIB milling. The result of this sample preparation provides an adequately smooth surface for EBSD. Electron backscatter diffraction is similar to XRD but in contrast to XRD it can detect each individual grain orientation. EBSD was carried out in the dual beam FEI Nova 600.

The resolution of electron back-scatter diffraction can be improved from tens of nanometres [5-6] to ~5 nanometres if

an electron transparent film is produced and positioned at 20º to the horizontal. Kikuchi patterns can be produced and collected from transmitted electrons from the underside of the sample. The experimental setup is shown schematically in figure 1. This increases the spatial resolution of EBSD which is advantageous for this study due to the relatively small grain sizes and defects such as twins present as well as localized changes of phase.

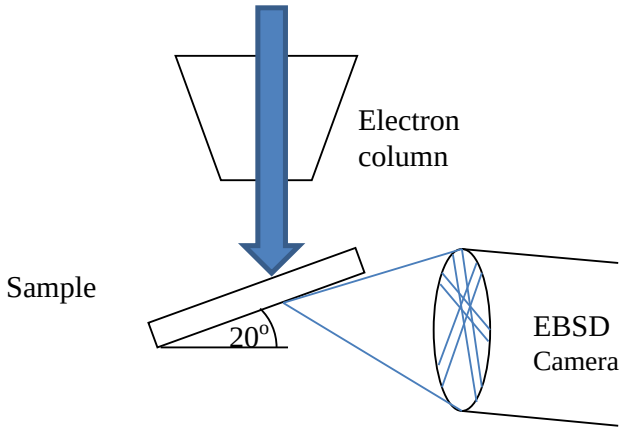

Fig. 1. A schematic diagram of the transmission electron backscatter diffraction (T-EBSD) setup

III. Results

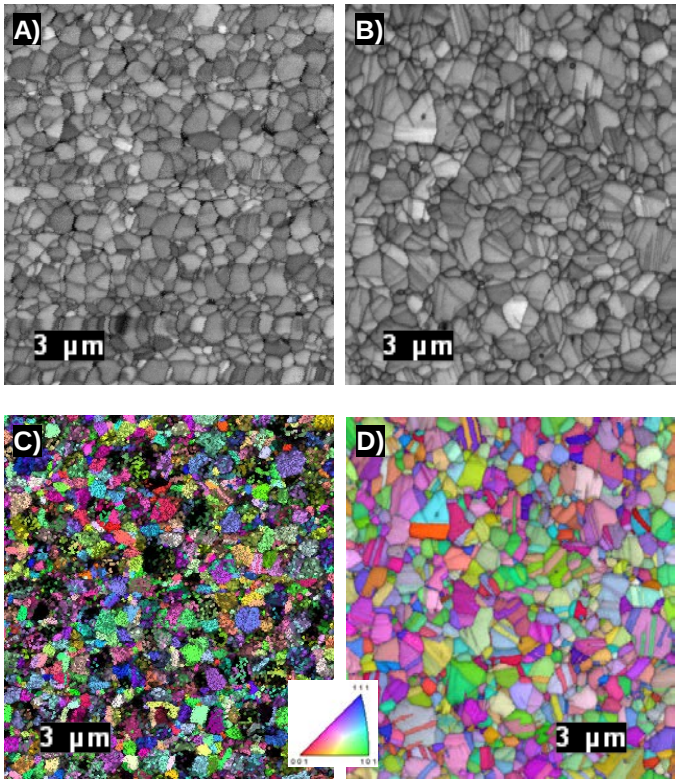

Fig. 2. EBSD derived Confidence index/Inverse pole figure maps of a) untreated and b) cadmium chloride treated cadmium telluride surface

Planar EBSD maps collected in untreated cadmium telluride samples were found to possess a significant number of mis-indexed points in the middle of grains. Figure 2 compares EBSD derived maps collected from treated and untreated cadmium telluride planar surfaces. The image quality maps shows that high quality Kikuchi patterns are collected from both samples. A comparison of the inverse pole figure/image quality composite maps shows speckling within the grains in the untreated sample and this feature is not present in the treated sample. A comparison of the confidence index/inverse pole figure composite maps shows that these intra granular speckles have a low confidence index and are consequently likely to be mis-indexed points. This behaviour is not observed in the treated samples.

To investigate the observed mis-indexing, high quality Kikuchi patterns were collected from various regions in the treated and untreated samples, a selection of which are compared in figure 3. It was found that some of the patterns in the untreated material did not index satisfactorily to the cubic cadmium telluride structure file.

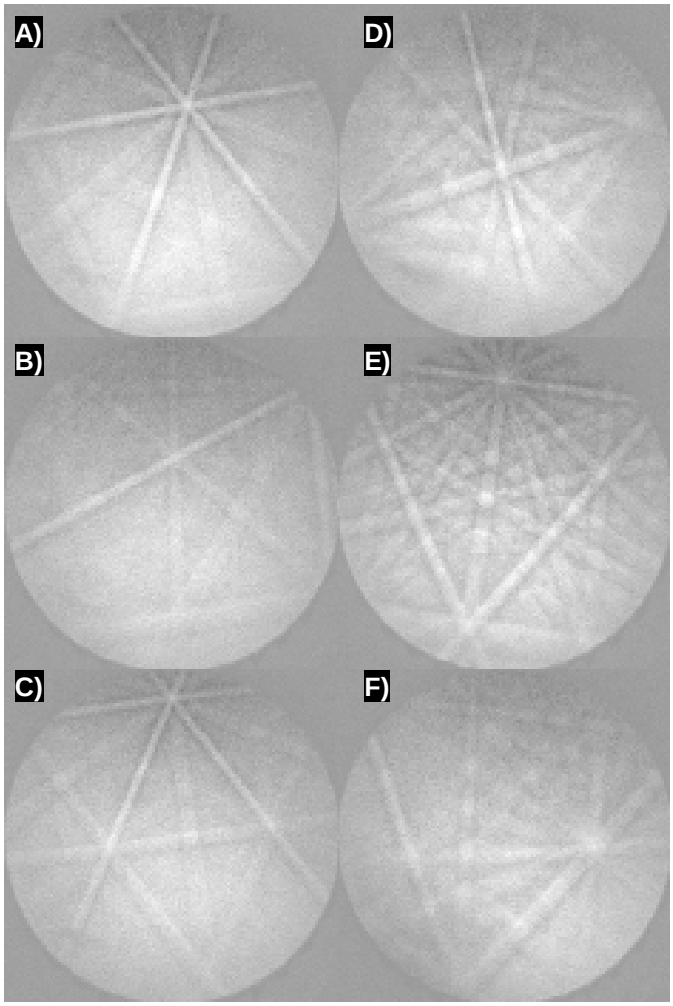

Fig. 3. Kikuchi patterns collected from a-c) an untreated, d-f) a treated cadmium telluride layer

Figure 4 compares XRD scans for the treated and untreated samples. The main differences observed are the broad peaks located at 39.2º corresponding to the (110) hexagonal peak and 42.7º corresponding to the (103) hexagonal peak in the untreated sample. The position of these peaks is consistent with the main peaks expected in the hexagonal cadmium telluride phase. These peaks could be from a phase with a fine grain size with Scherrer line broadening causing the peaks to appear broad [7].

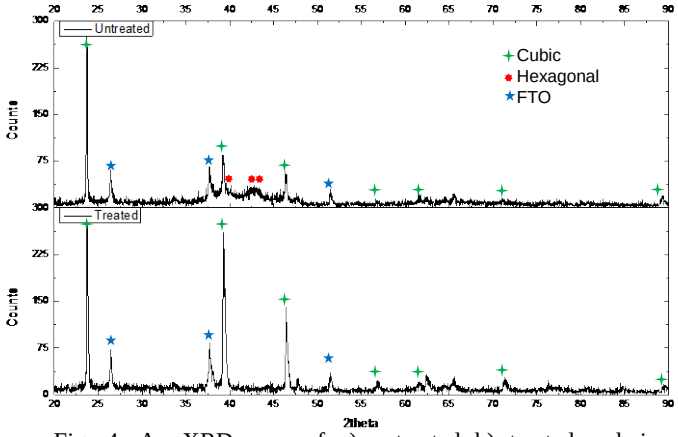

Fig. 4. An XRD scan of a) untreated b) treated cadmium telluride layer

The XRD data in figure 4 suggests that a hexagonal cadmium telluride phase is present in the untreated condition. To investigate this and map the phase distributions, a planar EBSD map of this sample was collected using both cubic and hexagonal phase files and the maps are shown in figure 5.

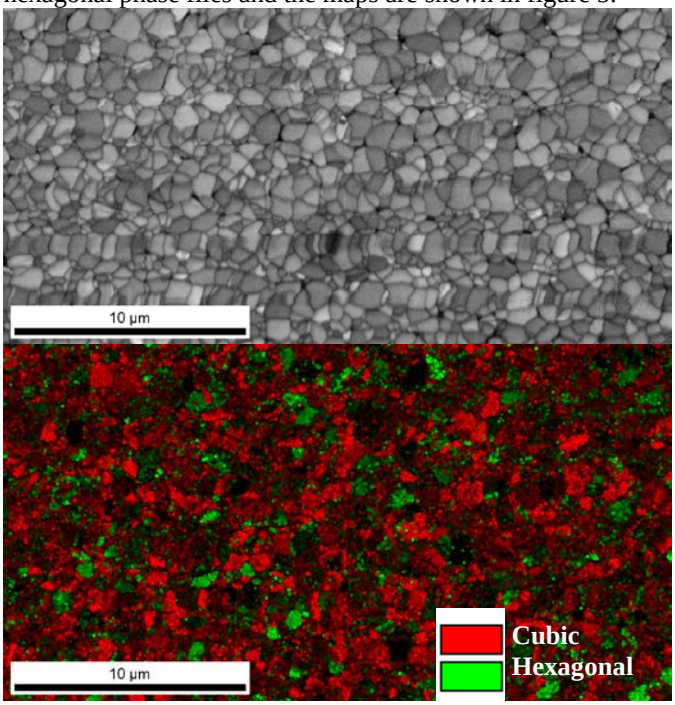

Fig. 5. EBSD derived Confidence index/Phase composite maps of the untreated cadmium telluride surface

These maps clearly show that in the untreated condition the material contains both cubic and hexagonal phases and a high confidence index is achieved in all intra-granular locations. Although this technique shows the distribution of phases, improved spatial resolution is needed to study this interesting result in more detail to reveal how the phases are distributed within a grain.

Figure 6 is derived from a TEBSD scan of a cross section of untreated cadmium telluride indexed against both cubic and hexagonal phase structure files. Figure 6a shows the image quality map overlaid with a phase map. Within the untreated cadmium telluride, some grains have formed bands of hexagonal material. These bands are usually 20 - 100 nm thick and run across the width of the cadmium telluride grain approximately perpendicular to the growth direction.

Figure 6b shows a TEBSD phase map overlaid with a confidence index map. The bands of hexagonal phase are seen to index with high confidence index to the hexagonal phase structure file indicating that the hexagonal phase is embedded within the cubic grains.

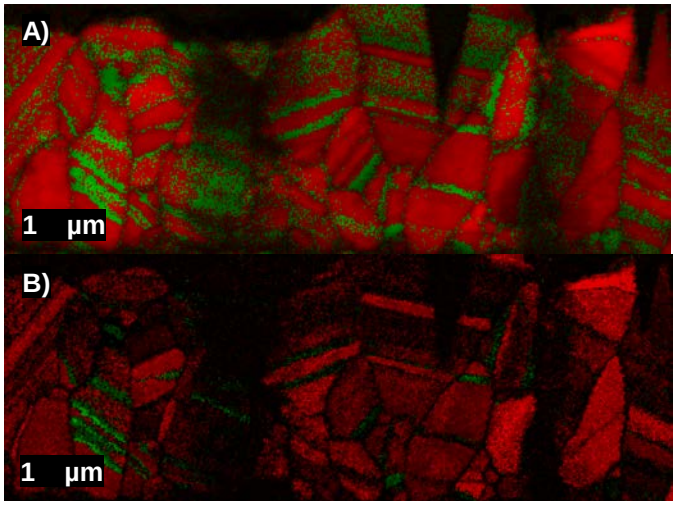

Fig. 6. High resolution TEBSD derived maps showing the distribution of the two phases, showing the cubic phase in red and hexagonal phase in green overlaid with a) image quality and b) confidence index

Observations from figure 5 show some grains appear to be hexagonal Wurtzite (shown in green) and some appear completely cubic. However in figure 6 this is proved to be an artefact of the planar EBSD geometry. As the cadmium telluride grains grow from the base up, bands of hexagonal material are deposited. The planar EBSD images a slice perpendicular to the growth direction. This plane intersects the Wurtzite band giving the illusion that the entire grain is hexagonal. T-EBSD in figure 6 shows the reality that only a localized area of the cadmium telluride grains exhibits the hexagonal Wurtzite structure, whereas most of the grain is cubic.

completely cubic. However in figure 6 this is proved to be an artefact of the planar EBSD geometry.

From the TEBSD analysis it has been shown that bands of hexagonal phase have formed within cubic cadmium telluride grains. Figure 7a shows a HRTEM image of the untreated cadmium telluride layer. This shows a high density of defects within the grain. The defects consist of stacking faults and twins, however the distribution is non-homogeneous. Two distinct regions of stacking faults every 2 atomic planes for is several atomic layers can be seen. The stacking in a perfect cubic lattice is AaBbCcAaBbCc… however as a plane missing from every sequence, the stacking sequence becomes AaBbAaBa… this is hexagonal Wurtzite packing. The hexagonal regions have been marked in figure 7a, which appear in bands and a schematic of the buried hexagonal phase with cubic phases either side is shown in figure 7b. This high density of stacking faults causes a shift from cubic material to hexagonal material. Therefore both phases are present within the same grain, as seen by TEBSD.

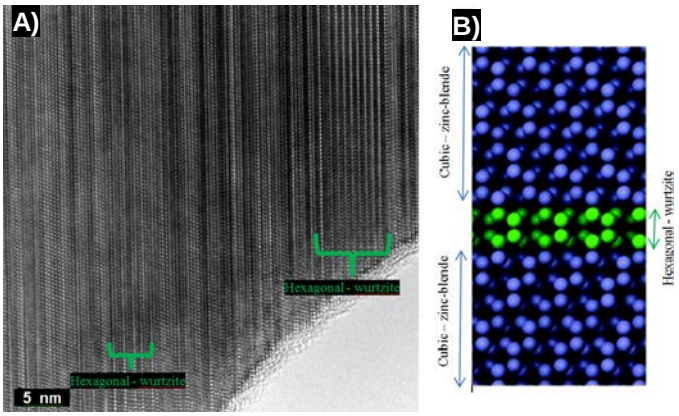

Fig. 7. a) A HR-TEM micrograph of a untreated cadmium telluride grain with highlighted hexagonal stacking highlighted, b) schematic of cubic and hexagonal stacked atomic layer.

Figure 8a shows a higher resolution T-EBSD phase map of an untreated cadmium telluride device. This map clearly shows the distribution of the two phases. Figure 8b shows a similar map taken from a treated cadmium telluride device. All areas index with a high confidence. Twin boundaries are observed in most cadmium telluride grains by a 60 degree orientation change. This indicates the twin boundaries in the cadmium telluride grains after the cadmium chloride are mainly $\sum 3$ twins. No twins were observed in the untreated cadmium telluride, due to the high density of stacking defects.

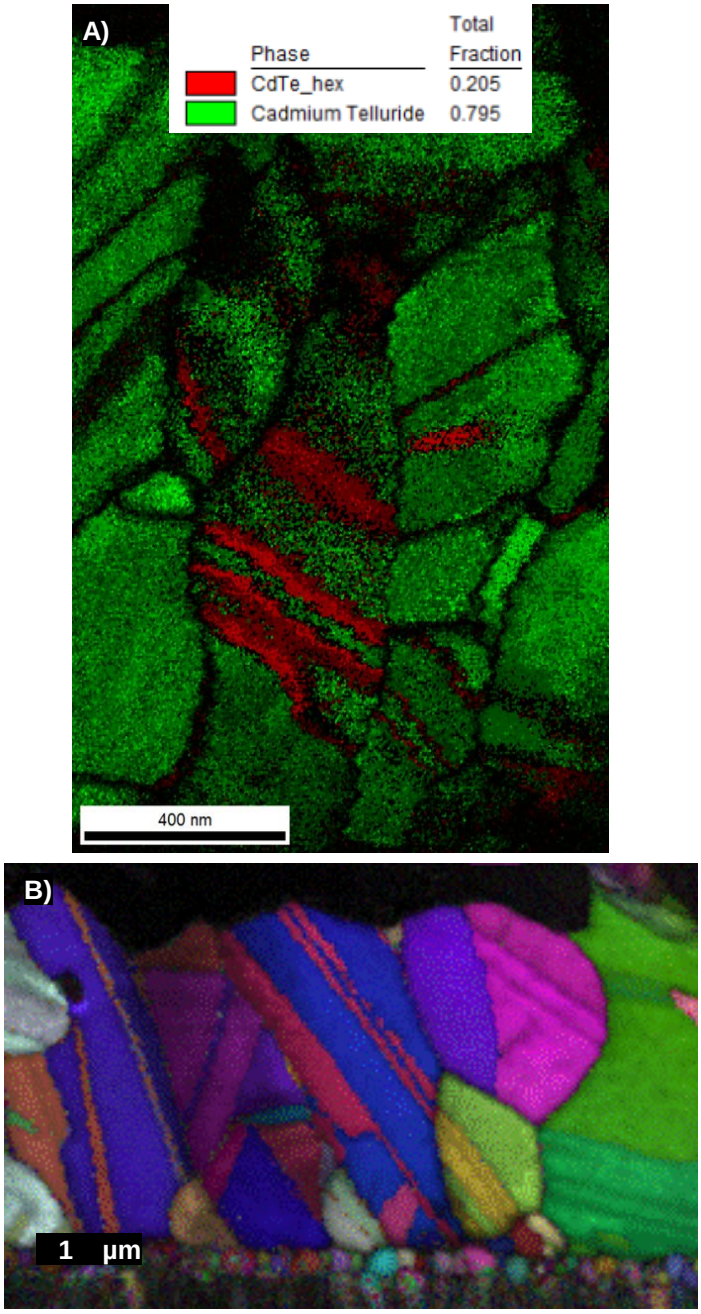

Fig. 8. EBSD derived maps showing a) phase/confidence index of an untreated CdTe cell b) inverse pole figure map of a treated device.

IV. Conclusions

TEBSD has been used to produce high resolution phase maps cadmium telluride solar cells for the first time, showing hexagonal areas within cubic cadmium telluride grains. This phenomenon has been observed in cadmium telluride grains prior to the cadmium chloride treatment. Cadmium telluride grains after the cadmium chloride treatment have recrystallized, forming pure cubic grains.

V. ACKNOWLEDGEMENTS

The Loughborough authors are grateful to UKERC for financial assistance through the EPSRC Supergen SuperSolar Hub and the CSU authors to the NSF I/UCRC and AIR programs.

VI. REFERENCES

[1]Haegel, N. M. *et al.* Terawatt-scale photovoltaics: Trajectories and challenges. *Science (80-.).* 356**,** (2017)

[2] J.M. Walls, A. Abbas, G. D. West, J.W. Bowers, P.J.M. Isherwood, P.M. Kaminski, B. Maniscalco, W.S. Sampath and K.L. Barth, "The Effect of Annealing Treatments on Close Spaced Sublimated Cadmium Telluride Thin Film Solar Cells," MRS Online Proceedings Library, Volume 1493, mrsf12-1493-e04-02, January 2012.

[3] A. Abbas *et al*., "Cadmium chloride assisted re-crystallization of CdTe: The effect of the annealing temperature," *2013 IEEE 39th Photovoltaic Specialists Conference (PVSC)*, Tampa, FL, 2013, pp. 0356-0361.

[4] Barth, K.L.; Enzenroth, R.A.; Sampath, W.S "Advances in continuous, in-line processing of stable CdS/CdTe devices," Photovoltaic Specialists Conference, 2002. Conference Record of the Twenty-Ninth IEEE, vol, no. pp. 551- 554, 19-24 May 2002

[5]Trimby, Patrick W. "Orientation mapping of nanostructured materials using transmission Kikuchi diffraction in the scanning electron microscope." Ultramicroscopy 120 (2012): 16-24.

[6] Keller, R. R., and R. H. Geiss. "Transmission EBSD from 10 nm domains in a scanning electron microscope." Journal of Microscopy 245.3 (2012): 245-251

[7] H.P. Klug & L.E. Alexander, *X-Ray Diffraction Procedures*, 2nd Ed., John Wiley & Sons Inc., 1974, p 687-703, ISBN 978-0-471-49369-3